Application of fixed delay Michelson interferometer for Radial Velocity measurement

Kai Zhang *[a,b,c], Mingda Jiang [a,b,c], Yongtian Zhu [a,b]

[a] National Astronomical Observatories/Nanjing Institute of Astronomical Optics & Technology, Chinese Academy of Sciences, Nanjing 210042,China;

[b] Key Laboratory of Astronomical Optics & Technology, Nanjing Institute of Astronomical Optics & Technology, Chinese Academy of Sciences, Nanjing 210042,China;

[c] Graduate University of Chinese Academy of Sciences, Beijing 100049, China.

ABSTRACT

Fixed Delay Michelson Interferometer (FDMI) also called Wide-Angle Michelson Interferometer (WAMI) is different from conventional Michelson interferometer. Its fixed delay is not only useful to widen the field of view, but also improve the accuracy of RV measurement. So it's widely known that works well on upper atmospheric wind study by measuring the Doppler shift of single emission lines. On the other hand, a new technique called External Dispersed Interferometry (EDI) can efficiently overcome the fundamental limitation of narrow bandpass of interferometer by combination between FDMI and post-disperser. The related instruments have been successfully used in the exoplanet exploration field. In this paper, the FDMI concept and its application in these two fields are reviewed, and a major astronomical project in China, which is developing a multi-object exoplanet survey system (MESS) based on FDMI, is introduced.

Keywords: Fixed Delay Michelson Interferometer, Radial Velocity, Upper Atmospheric Wind, Exoplanet Exploration

1 INTRODUCTION

In familiar astronomical physics field, it's widely known that Radial Velocity (RV) approach is the most common way for exploring extra-solar planet because of Doppler Effect. In this approach, spectrograph is a key instrument for high-precision RV measurement. But with increasing requirement about exploration efficiency and precision, building more high-resolution spectrographs and larger aperture telescopes is not the best solution but just a traditional one. Many great astronomers and researchers all over the world try to change this state, e.g. David J. Erskine work at Lawrence Livermore National Laboratory (LLNL) invented an improved RV approach, called External Dispersed Interferometry (EDI) technique in 1997 [1]. The corresponding RV precision of medium-resolution spectrograph can be enhanced 2~6 times by this novel technique [2]. Actually, the reason why the enhancement can be achieved is the combination between a Fixed Delay Michelson Interferometer (FDMI) and a spectrograph. In 2002, Erskine, Jian Ge and their colleagues integrated a prototype of Exoplanet Tracker (ET) with KNPO 2.1m telescope. In 2005, a new exoplanet HD 102195b confirmed by ET on KNPO 2.1m telescope was named ET-1 to commemorate its first exoplanet detection [3] [4]. After this

* kzhang@niaot.ac.cn; phone 86-25-85482281; Fax 86-25-85405562

Ground-based and Airborne Instrumentation for Astronomy III, edited by Ian S. McLean, Suzanne K. Ramsay, Hideki Takami, Proc. of SPIE Vol. 7735, 773555 · © 2010
SPIE · CCC code: 0277-786X/10/$18 · doi: 10.1117/12.856238

success, Erskine and Jerry Edelstein proposed to develop a TripleSpec Exoplanet Discovery Instrument (TEDI) on the Palomar 200” telescope. It joins EDI with a medium-resolution, near IR (0.9-2.4um) echelle spectrograph, and is planed to observe cool stays [5]. On the other hand, Prof. Ge and his team in Florida University finished the integration of the next generation of ET, W. M. Keck Exoplanet Tracker, and SLOAN Digital Sky Survey (SDSS) 2.5m telescope at APO in 2005 [6]. This multi-object instrument finally has a wavelength coverage of 70nm, 60 fibers and 4K×4K CCD at a spectral resolution of R~10,000. Both Keck ETs have been included as a part of the Multi-object APO Radial Velocity Exoplanet Large-area Survey (MARVELS) action in SDSS III program since 2008. At the same time, more and more improvement is also under the development by more and more astronomers.

FDMI has been applied to exoplanet exploration only for a short time, however, has been applied into Upper Atmospheric Winds (UAW) field since 1960s or earlier. In 1966, R. L. Hilliard and G. G. Shepherd successfully showed an improved Michelson interferometer based on field-compensated principle [7] [8] to measure Doppler line widths [9] [10]. FDMI, which is also called Wide-angle Michelson Interferometer (WAMI), had been increasingly applied into UAW measurement since the success of Hilliard and Shepherd. Some representative instruments developed in the past 40 years are list as follows:

(1) In 1985, G. G. Shepherd, William A. Gault and their staff published a Wide-Angle Michelson Doppler Imaging Interferometer (WAMDII) for spacelab to measure the upper atmospheric winds and temperatures. It’s not only an achromatic field-compensated instrument with good thermal stability, but also the mature represent of an integral FDMI system [11].

(2) On September 12, 1991, the WIND Imaging Interferometer (WINDII) sponsored by the Canadian Space Agency (CSA) and the French Centre National d’ Etudes Spatiales was launched on the UARS by NASA. It measures wind, temperature and emission rate over the altitude range 80 to 300Km by using the visible airglow emission. This instrument is regard as the milestone of FDMI development [12].

(3) Since 1998, Stratospheric Wind Interferometer For Transport studies (SWIFT) has been developed by the cooperation of CSA, the Canadian Centre for Research in Earth and Space Technology (CRESTech) and York University. It’s an instrument very similar to the WINDII on UARS but operates in the mid-IR band. And it’s included as a part of a mini-satellite mission Chinook of CSA [13].

(4) In 2001, W. E. Ward and his colleagues published a visible/near-IR interferometer, Wave Michelson Interferometer (WaMI), for observing middle atmosphere dynamics and constituents. It’s included as a part of the Waves Explorer mission (G, Swenson, P. I.), which is proposed for NASA’s MIDEX program [14].

(5) In 2002, W. E. Ward and his colleagues introduced another imaging interferometer, Dynamics atmosphere Mars Observer (DYNAMO), for satellite observations of wind and temperature on Mars [15].

In addition, the common advantage of these above instruments in both science fields is that improves the traditional RV method by measuring the interference phase shifts. According to the equation (1) [2], fixed delay τ is obviously a RV amplifier. But due to the fundamental limitation of narrow bandpass, only single emission radiated from upper atmosphere is used for RV measurement.

$$v = \frac{c\lambda}{\tau}\frac{\Delta\phi}{2\pi} \tag{1}$$

Where C is the light rate in vacuum; λ is the wavelength; $\Delta\phi$ is the phase shifts caused by Doppler Effect; τ is the fixed delay, also called optical path difference (OPD) between the both interference arms.

2 MULTI-OBJECT EXOPLANET SURVEY SYSTEM

This new technique EDI and related FDMI have been impressive in China, although the newest and most decisive observational result has not been published in the world. Moreover, the Chinese Large sky Area Multi-Object fiber Spectroscopy Telescope (LAMOST) [16] has technically been the most powerful survey telescope with large aperture and big viewing field since the successful official blessing in 2009. Its exciting property includes a 4m aperture and a 5° field of view, which accommodate as many as 4000 optical fibers, and 16 multi-object Low-medium Resolution Spectrometers (LRS) [17]. The numbers of fibers and spectrometers give us an overwhelming superiority in multi-object exoplanet exploration. A major astronomical project, which is developing a Multi-object Exoplanet Survey System (MESS), has been actively carried out by cooperation between Nanjing Institute of Astronomical Optics and Technology (NIAOT) and National Astronomical Observatories of China (NAOC) under the fund support of Joint Fund of Academy, which is set up by National Natural Sciences Foundation of China (NSFC) and Chinese Academy of Sciences (CAS). The purpose is that further enhance the RV precision through applying the EDI technique into the existing LRS.

Each LRS, which works in medium-resolution mode, is a multi-fiber VPH grating spectrometer with 250 fibers and two detecting parts (Red and Blue arm). The spectral resolution is about 5,000 covering 5,100-5,400 Å (Blue arm) and 8,300-8,900 Å (Red arm) respectively. Each fiber connecting to the focal plane has a aperture of 0.32mm and a F number of 4. And spectrum in different arm is separately gathered by a corresponding 4K×4K CCD camera. In MESS, a multi-object FDMI will be inserted between the telescope and a LRS. The focal plane of telescope is connected to the interferometer by fibers, and then the output interfering beam directly transmits into spectrometer through the slit. Finally, the interference spectrum will be imaged on the CCD, as follow shown.

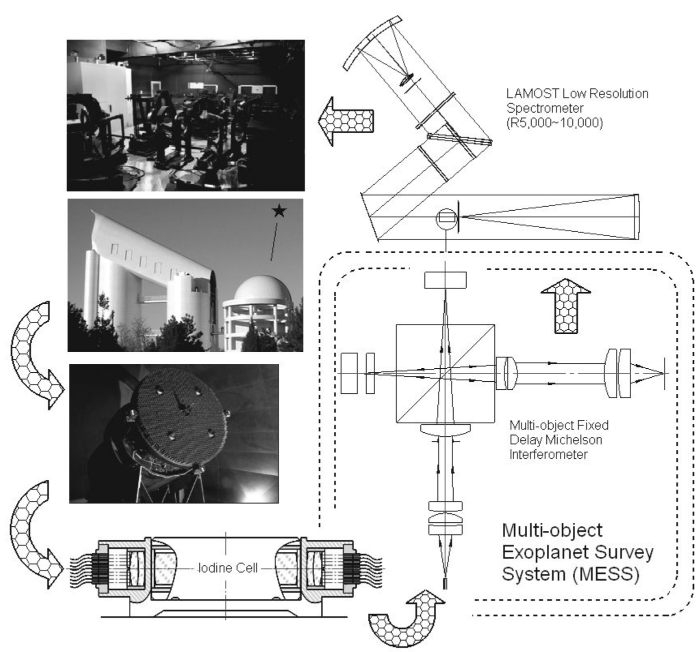

Fig.1 Schematic drawing of MESS

According to the EDI principle [18] [19], an interference spectrum is created by externally dispersing the interference comb, and then a new kind of moiré pattern is produced by heterodyning the interferometer spectrum with stellar absorption lines, as figure (2). So the Doppler shift along the slit direction becomes more obvious than the one along the dispersion direction. On the other hand, big viewing field of FDMI can gather more starlight than the conventional one and produce a phase-uniform or phase-slant interference spot. These are key points of EDI technique. After early research [20], a feasibility experiment was finished in the spectral lab. Figure (3) shows some experimental pictures of platform and interference spectrum.

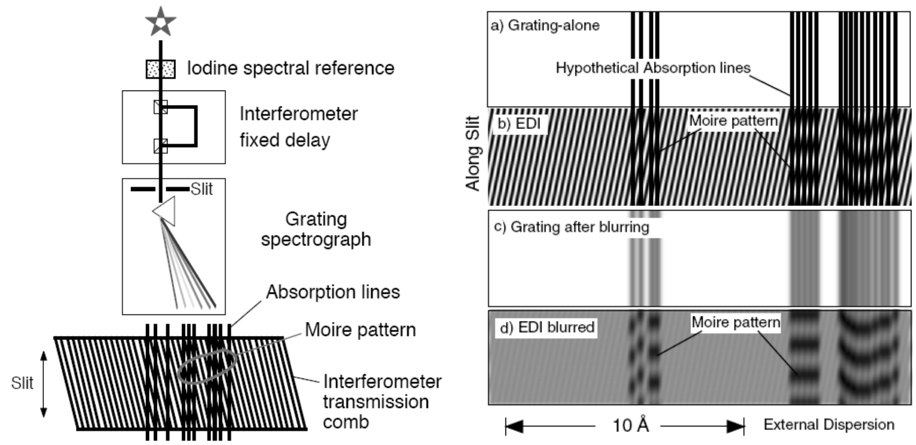

Fig.2 Principle of EDI [19] and model of moiré fringe [18]

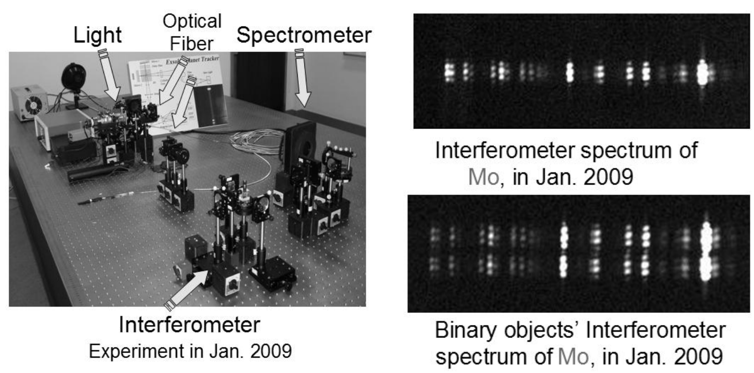

Fig.3 Pictures of MESS feasible experiment

For spectrometer, the interference spectrum is two-dimension spectral pattern, including slit and dispersion directions. In order to resolute 3~5 fringes along the slit direction, the number of fibers per MESS decreases from 250 to 30 at most. Though there will be only about 30 objects per spectrometer, LAMOST still have powerful observational ability for multi-object observation, which is equivalent to 480 objects in total. Compared to the original structure of LRS, the existing slit component will be replaced by a multi-object FDMI. And a triple-object FDMI prototype is under the development right now, as figure (4).

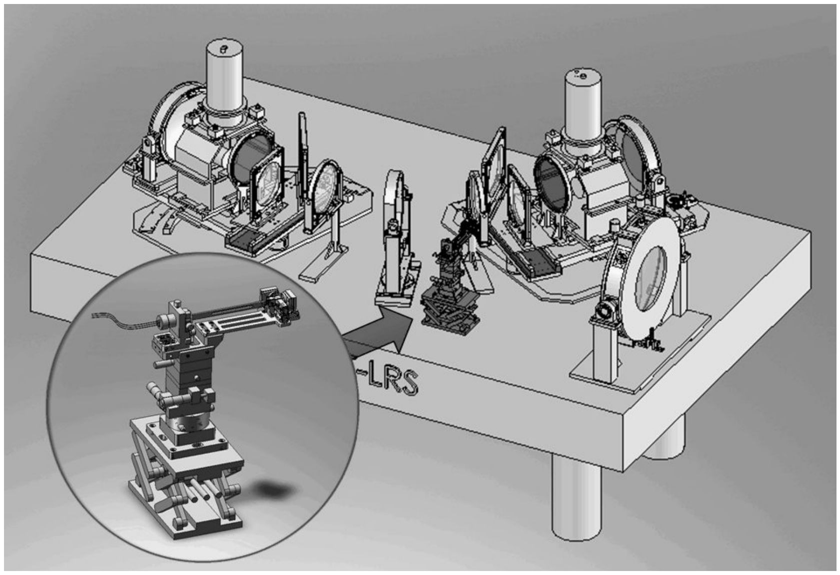

Fig.4 Overall structure of triple-object MESS prototype

3 DESIGN OF FDMI

In this prototype, the current interference component is still an adjustable experimental one that contains a non-polarized cubic beam splitter (BS), two high-reflection mirrors and a parallel plate. Because the interfering arms are composed of the glass plate and an air gap, the thermal stability and achromatic feature can't meet the practical requirement. At present, a better component with the stable achromatic and thermal performance is under the development. Besides of fixed delay and field compensation, the achromatic thermal stability and some fabricating problems are also seriously concerned.

The FDMI design principle [18] [21] is gradually more perfect through all kinds of improvement. Firstly, fixed delay also called Optical Path Difference (OPD) is the most important feature of interferometer. For conventional Michelson Interferometer (MI), the OPD sensitively varies with the change of incident angle. However, the OPD of FDMI is able to approximate the fixed one τ_o, as equations (2), (3).

$$\tau = 2(n_1 L_1 Cos\varphi_1 - n_2 L_2 Cos\varphi_2) \tag{2}$$

$$\tau_o = 2(n_1 L_1 - n_2 L_2) \tag{3}$$

Where L_1, L_2 are respectively the lengths of different arms, n_1, n_2 are respectively the refractive indexes of different arms, φ_1, φ_2 are respectively the incident angles in different arms.

Field compensation means that make the OPD fixed with various incident angles. According to the field-compensated principle, an approximate equation is got by expand all the terms of $Sin\varphi$ till the fourth order and ignore higher order terms. When the $Sin^2\varphi$ term can be set to zero by choosing a suitable pair of arms' materials, it allows a much larger acceptance angle for the interferometer, as follow shown. When the higher order terms are also approximate to zero, it achieves the fully field compensation.

$$\tau = \tau_o - \left(\frac{L_1}{n_1} - \frac{L_2}{n_2}\right) Sin^2\varphi - \left(\frac{L_1}{n_1{}^3} - \frac{L_2}{n_2{}^3}\right)\frac{Sin^4\varphi}{4} \tag{4}$$

$$w = \frac{L_1}{n_1} - \frac{L_2}{n_2} = 0 \tag{5}$$

Achromatic feature, which is certainly different from the one in aberration theory, means that OPD is the same in a certain wave band. A derivative on wavelength λ can be used to evaluate its achromatic performance. When a suitable glass pair was chosen, the OPD difference caused by different wavelength is enough small to be accepted, as follows:

$$\frac{\partial w}{\partial \lambda} = 0 \tag{6}$$

Thirdly, good thermal stability is another important requirement. Some derivatives on temperature *T* are also set to evaluate its performance, as follow shown.

$$\frac{\partial \tau}{\partial T} = 0 \tag{7}$$

$$\frac{\partial^2 \tau}{\partial T \partial \lambda} = 0 \tag{8}$$

Absolutely, it's difficult that all the features shown in equations (5)-(8) are fully finished by choosing glass-pair from the existing glass categories. For balance during the above conditions, the glass-choosing process is defined to be four steps:

(1) Build an independent glass database, which is composed of a series of individual data units. Every data unit has three parameters, including a gain coefficient of refractive index versus wavelength α, a thermal line expansion coefficient β and a gain coefficient of refractive index versus temperature γ, as follows:

$$\alpha = \frac{1}{n}\frac{\partial n}{\partial \lambda} \tag{9}$$

$$\beta = \frac{1}{l}\frac{\partial l}{\partial T} \tag{10}$$

$$\gamma = \frac{1}{n}\frac{\partial n}{\partial T} \tag{11}$$

(2) In the condition of the required OPD and field compensation, the second step is a further filter that contains five conditions for the achromatic and thermal immunity, as the following equation group (20). Building an OPD database of glass-pairs is used as a directly effective test method for optimized means. Every data unit called glass cube is a three-dimension array, which has different OPD values respectively on wavelength, temperature and incident angle. By the using of this database, the OPD error of different glass-pair is easily compared. But the number of glass categories is bigger than 5,000 so that the analysis becomes time-consuming. So this database is more useful in test process.

$$\left.\begin{array}{l} \dfrac{\partial w}{\partial \lambda} = 0 \\ \dfrac{\partial w}{\partial T} = 0 \\ \dfrac{\partial \tau_o}{\partial \lambda} = 0 \\ \dfrac{\partial \tau}{\partial T} = 0 \\ \dfrac{\partial^2 \tau}{\partial T \partial \lambda} = 0 \end{array}\right\} \tag{12}$$

(3) Another means is a further optimized process about weighting function. The function shown in equation (13) contains the independent errors of the above five conditions $\delta w_\lambda, \delta w_T, \delta\tau_\lambda, \delta\tau_T, \delta\tau_{\lambda/T}$ and a group of weights a_1, a_2, a_3, a_4, a_5. The cooperation between the function and OPD database is a close loop for choosing the glass-pair. In this close loop, a small group of glass-pairs is easily got by adding a variable weight group into weighting function, and then the OPD database is used to test if the weight group is suitable. Finally, a small group of candidates is obtained.

$$Wn = a_1\delta w_\lambda + a_2\delta w_T + a_3\delta\tau_\lambda + a_4\delta\tau_T + a_5\delta\tau_{\lambda/T} \tag{13}$$

(4) In addition, defocusing effect was proposed as an adjusting optimization by H. H. Zwick and G. G. Shepherd [22]. Under the inspiration of defocusing effect, an active OPD error is also used as another optimization. The acceptable OPD error is necessarily in a certain range and the OPD error curve versus incident angle is usually monotone increasing, so the plus-minus acceptable error range is not fully used until bends the curve by adding a small OPD error ε, as the following equation (14). The figure (5) shows an example of glass-pair, N-LAK34 / BAF10. The fixed delay is defined to be 1mm and the max acceptable OPD error is defined to be ± 0.05 waves @527.4nm.

$$\tau_o = 2(n_1 L_1 - n_2 L_2) + \varepsilon \tag{14}$$

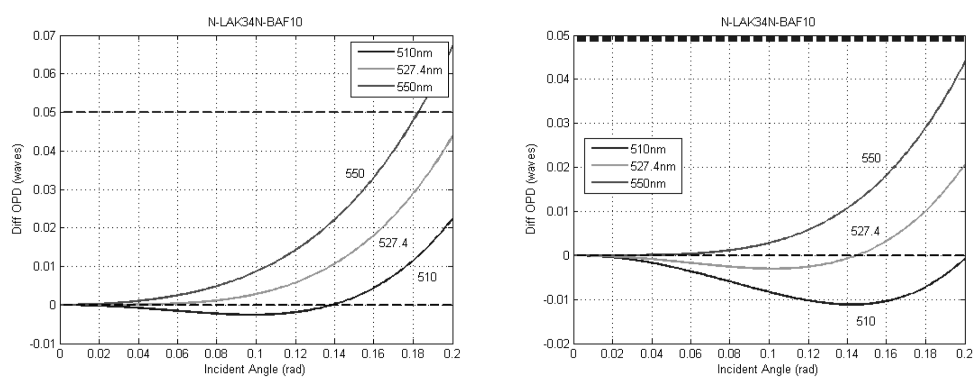

(a) Without Defocusing Effect (b) With Defocusing Effect

Fig. 5 OPD error curve of a glass-pair: N-LAK34 / BAF10.

After the above process, the fabricating condition is concerned, especially the coating of beam splitter, because the conventional non-polarized splitting film possesses only a small field of view. A conventional splitting film with a prime incident angle of 45° is simulated as the following figure 6(a). The result is that the light polarization and transmission through the splitting film sharply drop when the incident angle is different from the prime one, such as 35° and 55° shown in figure 6(b), 6(c). Therefore, a suitable splitting film is worth concerning in the FDMI design process, and maybe the other fabricating problem need more considering, e.g. a hexagonal BS will take place of the cubic one in order to avoid the Brewster angle [23].

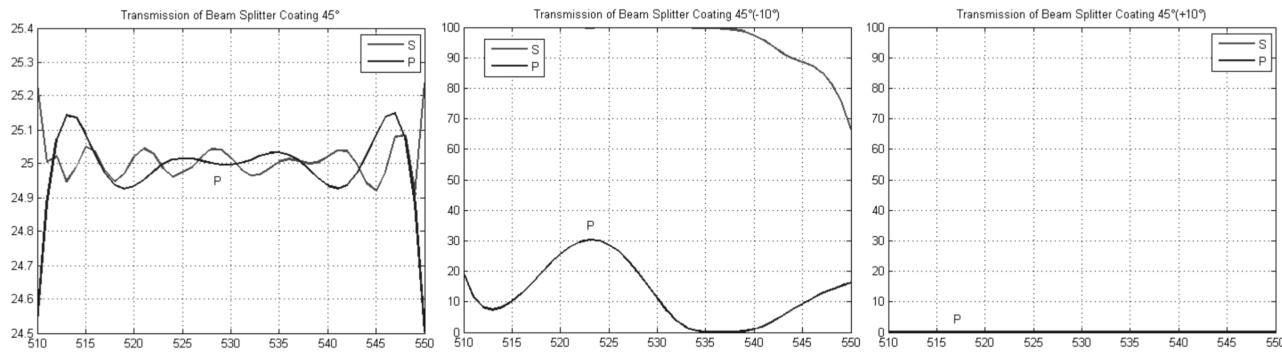

(a) (b) (c)

Fig.6 simulation of conventional splitting film

4 CONCLUSION

According to the review of FDMI development, it plays an important role in both UPW study and exoplanet exploration fields. And a practice FDMI possesses four features, such as fixed delay, field compensation, achromatic feature and thermal stability. Moreover, the actual fabricating process also directly influents the interferometer performance, such as the output beam polarization and fringe visibility. The FDMI in MESS project is not only required to meet these features, but also possess the multi-object function and compact structure.

This work is the first stage of MESS project. In this stage, it includes the overall integration of experimental instrument, the development of data processing program. Because of the existing limit, it’s more complicated and difficult to finish it, such as center obscuration, arc-shape slit, the fiber coupling problem in iodine cell component and the interchangeable function with slit component, etc.

5 ACKNOWLEDGEMENTS

MESS is being performed by corporation between NIAOT and NAOC under the fund support of Joint Fund of Astronomy, which is set up by NSFC and CAS (No. 10978004). Here, thank my tutor Prof. Yongtian Zhu and Prof. Gang Zhao, Liang Wang work at NAOC to help finishing the above work in the past study.

REFERENCES

[1] D. Erskine and J. Ge, “Novel Interferometer Spectrometer for Sensitive Stellar Radial Velocimetry”, ASP Conf, 195, 501-507 (2000).

[2] J. Ge, D. Erskine and M. Rushford, “An Externally Dispersed Interferometer for Sensitive Doppler Extra-solar Planet Searches”, PASP 114, 1016-1028 (2002).

[3] J. van Eyken, J. Ge, etc. “Results from upgrade to the Radial Velocity Instrument ET at the KPNO 2.1m”, Proc. SPIE, 5492, 445-451 (2004).

[4] J. Ge, J. van Eyken, etc. “The first extrasolar planet discovered with a new generation high throughput Doppler instrument”, Astrophysical J. 648, 683-695 (2006).

[5] J. Edelstein, M. W. Muterspaugh, et al. “TEDI: the TripleSpec Exoplanet Discovery Instrument”, Proc. SPIE 6693, (2007).

[6] J. Ge, J. van Eyken, et al. “An All Sky Extra-solar Planet Survey with New Generation multiple Object Doppler Instruments at Sloan Telescope”, RevMexAA (Serie de Conferencias) 29, 30-36 (2007).

[7] L. Mertz, “Transformations in Optics”, 18 (1965).

[8] P. Connes, “ ”, Rev. Opt. 35, 37 (1956).

[9] R. L. Hilliard and G. G. Shepherd, “Wide-angle Michelson Interferometer for Doppler Line Widths”, J. Opt. Soc. Am 56 (3), 362-369 (1966).

[10] R. L. Hilliard and G. G. Shepherd, “Upper Atmospheric Temperature from Doppler Line Widths, Planet”, Space Sci. 14, 383 (1966).

[11] G. G. Shepherd, W. A. Gault, etc. “WAMDII: wide-angle Michelson Doppler imaging interferometer for spacelab”, Appl. Opt. 24 (11), 1571-1584 (1985).

[12] W. A. Gault, G. G. Shepherd, etc. “The Wind Imaging Interferometer (WINDII) on the Upper Atmosphere Research Satellite”, Proc. SPIE 1745, 54-60 (1992).

[13] W. Gault, I. McDade, etc. “SWIFT：An infrared Doppler Michelson interferometer for measuring stratospheric winds”, Proc. SIPE 4540, 476-481 (2001).

[14] W. E. Ward, W. A. Gault, etc. “The Waves Michelson Interferometer: A visible/near-IR interferometer for observing middle atmosphere dynamics and constituents”, Proc. SPIE 4540, 100-111 (2001).

[15] W.E. Ward, W.A. Gault, etc. “An imaging interferometer for satellite observations of wind and temperature on Mars the Dynamics Atmosphere Mars Observer, the Dynamics Atmosphere Mars Observer (DYNAMO)”, Proc. SPIE 4833, 226-236 (2002).

[16] Dingqiang Su, Xiangqun Cui et al. “Large-sky-area multi-object fiber spectroscopic telescope (LAMOST) and its key technology”, Proc. SPIE 3352, 76 (1998).

[17] Yongtian Zhu, Zhongwen Hu, et al. “A multipurpose fiber-fed VPHG spectrograph for LAMOST”, Proc. SPIE 6269, (2006).

[18] D. Erskine and J. Edelstein, “High-Resolution Broadband Spectral Interferometry”, Proc. SPIE 4854, 1-12 (2002).

[19] D. Erskine, “An Externally Dispersed Interferometer Prototype for Sensitive Radial Velocimetry: Theory and Demonstration on Sunlight”, ASP 115, 255-269 (2003).

[20] Zhang Kai, Zhu Yongtian et al. “Study on the Space-Time Coherence of Fixed Delay Michelson Interferometer”, APS (Acta Photonic Sinica of China) 37 (Sup. II), 228-231 (2008).

[21] Suvrath Mahadevana, J. Gea, et al. “Design of a stable fixed delay interferometer prototype for the ET project”, Proc. SPIE 5492, 617-623 (2004).

[22] H. H. Zwick and G. G. Shepherd, “Defocusing a Wide-Angle Michelson Interferometer”, Appl. Opt. 10 (11), 2569-2571 (1971).

[23] J. A. Dobrowolski, F. C. Ho and A. Waldorf, “Beam Splitter for a wide-angle Michelson Doppler imaging interferometer”, App. Opt. 24 (11), 1585-1588 (1985).